Sekiguchi and Sato *Appl Adhes Sci (2017) 5:8*
DOI 10.1186/s40563-017-0086-8

Applied Adhesion Science

RESEARCH Open Access

Experimental investigation of the effect of tip shape in gecko-inspired adhesive devices under asymmetric detachment

Yu Sekiguchi* and Chiaki Sato

*Correspondence:
sekiguchi.y.aa@m.titech.ac.jp
Institute of Innovative Research (IIR), Tokyo Institute of Technology, 4259 Nagatsuta-cho, Midori-ku, Yokohama, Kanagawa 226-8503, Japan

Abstract

Gecko's foot hairs exhibit significant frictional anisotropy that enables a strong foot grip in a specific direction and an easy detachment in the opposite direction. In this study, we fabricate adhesive devices with frictional anisotropy mimicking gecko's foot hair based on oblique micro-beam arrays. The devices adhesion force is strongly anisotropic along the beam tilting direction and depends on the stress distribution at the contact area which, in turn, is affected by the geometry of the beam tips. This dependence is investigated by fabricating and testing micro beam arrays with various tip shapes.

Keywords: Bio-inspired, Dry adhesion, Biomimetics, Reversible adhesive device, Gecko

Background

It is usually challenging to achieve surfaces that are highly adhesive, yet can be detached easily. Geckos' foot hairs, however, can be easily detached from a surface even though they adhere to it strongly enough to hold the animal's body against gravity. Inspired by Nature, a combination of strong adhesion and easy detachment in adhesion system can be achieved and the possibility of reversible adhesion will be opened up.

Geckos' ability to climb vertical walls and hang upside-down on ceilings have attracted the attention of numerous scientists who, through careful observations, have linked these remarkable properties to microscopic hairs present on the surface of gecko's foot [1–4]. These findings were corroborated by measurements of the adhesive force of a single gecko foot hair [5]. Insects, such as beetles, also use foot hairs to improve their grip on surfaces [6, 7]. Several devices mimicking these foot hairs were fabricated, which showed improved adhesive properties [8–14].

In particular, a mushroom-like structure exhibited strong adhesive behavior by equalizing the stress distribution at a contact tip [15–19]. In contrast, an asymmetric stress distribution lowers the detachment force. When a tangential force is applied, a moment is generated in the structure and the stress at the contact area is asymmetrically distributed. The stress at the contact edge increases with the applied moment until the stress is reached at which point the detachment occurs [20]. Hence, the detachment force decreases when the moment increases, and the control of the moment is an important

factor for the reversible attachment and detachment processes. The detachment mechanism of straight beam adhesive devices has been investigated by analyzing the stress distribution at the contact tip [21–23].

The moment acting on the structure, and hence the detachment condition, depends on the pulling angle. When the adhesive structure is vertical, the detachment force is a symmetric function of the pulling angle [22]. However, when the structure is tilted, the relationship between the detachment force and the pulling angle becomes asymmetric. Specifically, the detachment force increases in the direction of the structure tilt and decreases in the opposite direction [23]. Therefore, this asymmetry arises from the inclination of the structure, and the adhesion strength can be controlled by changing the angle of the force. In this paper, the effect of tip shape on the asymmetric of the detachment force is experimentally investigated by fabricating tilted beam arrays with various tip shapes.

Methods

Device preparation

The manufacturing process of oblique beam arrays is shown schematically in Fig. 1a. A negative mold is composed of 3 parts: a milled metallic mold, a glass plate, and a glass fixing plate. A two-component silicone rubber (Base resin: KE-106, Hardener: CAT-RG, mixing ratio 10:1 by weight, Shin-Etsu Chemical Co., Ltd., Japan) was poured into the mold. The filled mold was transferred to a vacuum deaerator and subsequently cured at 140 °C for 3 h in an electric furnace. A representative images of the fabricated array is shown in Fig. 1b. Each device is composed of an array of 18 tilted beam structures. The tilting angle θ, height h, and width b, (see Fig. 1c), were 60°, 1 mm, and 2.5 mm, respectively.

Molds with different tip shapes were manufactured by mechanically milling the metallic mold using a micro end mill. Although, in principle, this technique allows fabricating molds with arbitrary tip shapes, in practice, oversized or complex tip shapes are difficult to release without damaging the cast. For this reason, only certain tip shapes, similar to those shown in Fig. 2, were fabricated successfully. The devices types 1, 2, and 3 in Fig. 2 exhibit tilted beam structures with thickness $H = 500$, 625, and 750 μm, respectively (denoted as S100%, S125%, and S150%, respectively). Devices types 4 and 5 have features similar to types 1–3, except that the tips are elongated at the rear (heel-like elongation) with the width W 1.25 and 1.5 times larger than Type 1, respectively (denoted as H125% and H150%). The type 6 device has beams with tips elongated at the front (toe-like

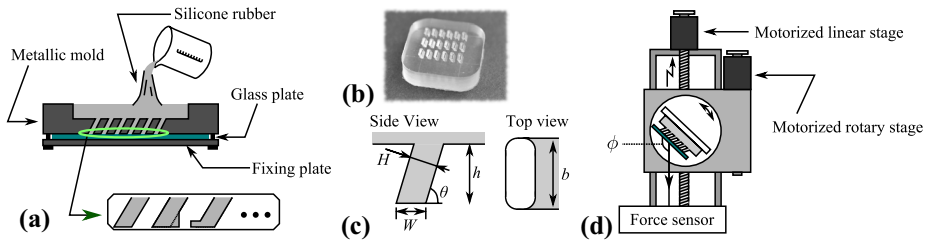

Fig. 1 **a** Schematics of the device fabrication process, **b** a picture of fabricated device, **c** a schematic of *side* and *top views* of each tilted beam structure, and **d** schematics of experimental setup for measuring device adhesion versus pulling angle

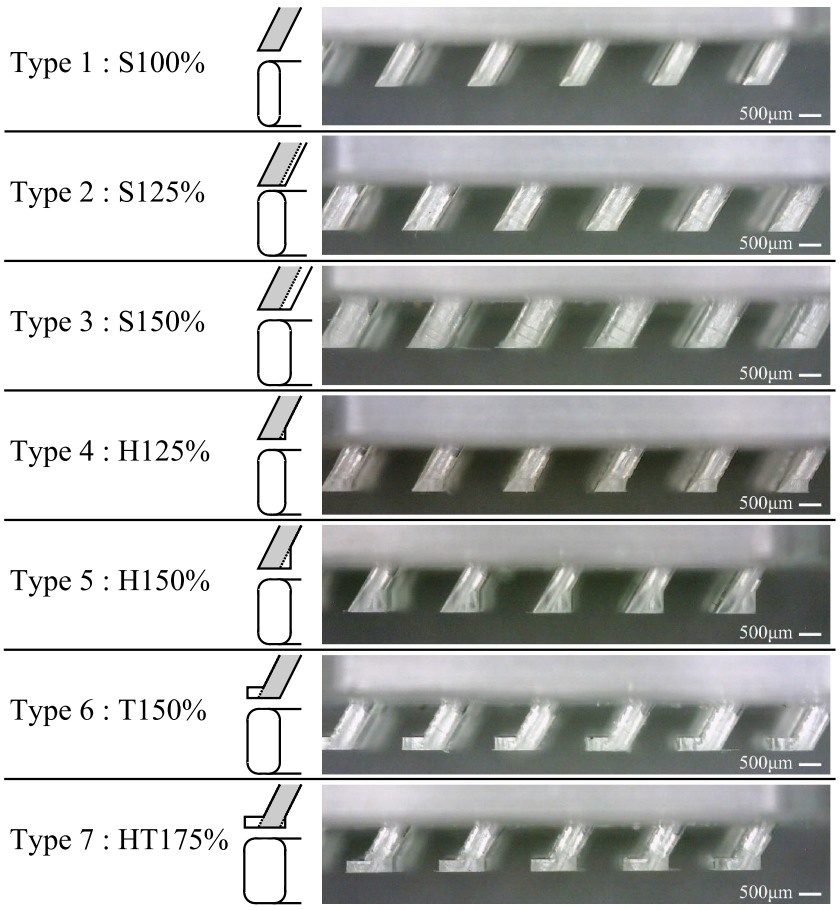

Fig. 2 Side view of various fabricated adhesive devices

elongation) and the width 1.5 times larger than Type 1 (denoted as T150%). Type 7 has tips elongated 1.25 times at the rear and 1.5 times at the front (i.e., 75% wider) compared with Type 1, (denoted as HT175%).

Experimental setup

The adhesive device was mounted on a motorized rotary stage, wiped clean with ethanol, and placed in contact with a glass plate (also previously cleaned with ethanol). Subsequently the device was turned to a predefined angle ϕ with respect to the vertical direction and moved upward with a motorized linear stage at a speed of 0.1 mm/s, as shown in Fig. 1d, until the glass plate detached from the device. The detachment force F was measured as a function of the pulling angle ϕ using a tuning-fork load sensor type electric balance (HJRII-2200, Shinko Denshi Co., LTD., Japan) with a resolution of 0.01 gf. The normal and tangential forces at the detachment were calculated using the equations: $F_{\mathrm{N}} = F \ \sin\phi$ and $F_{\mathrm{T}} = F \ \cos\phi$.

Adhesion criterion

Adhesion between the tip surface and the glass surface is due to intermolecular interactions, and detachment occurs when the maximum stress at the interface reaches the

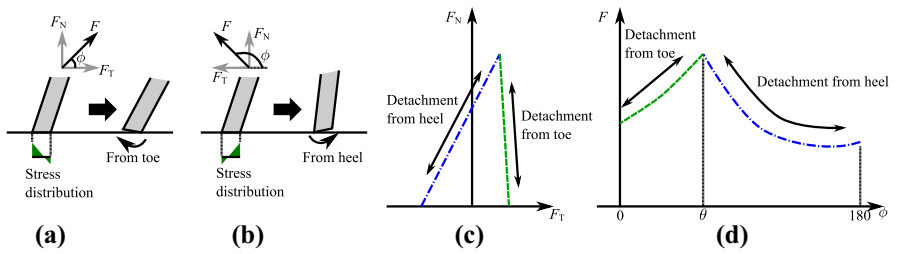

Fig. 3 Schematics of detachment in the case for **a** $\varphi < \theta$ and **b** $\varphi > \theta$. Additionally, the detachment conditions are shown in **c** F_N-F_T relation and **d** F-φ relation diagram

limiting stress of adhesion. In the case for the device with the straight structure, such as Type 1, 2, or 3, the detachment condition has been theoretically modeled and experimentally investigated [20, 22, 23]. When the force is applied in the beam tilting direction, i.e., $\phi = \theta$, there is no moment acting on the beams and the stress is symmetrically distributes at the contact point, thereby maximizing the detachment force. When the force is applied at an angle $\phi < \theta$, the stress at the front edge of the tip increases and the detachment occurs from the "toe" side, as shown in Fig. 3a. When the force is applied in the opposite direction, i.e., $\phi > \theta$, the stress at the rear edge of the tip increases and the detachment occurs from the "heel" side, as shown in Fig. 3b. The detachment condition as a function of the normal and tangential forces (F_N-F_T), and the pulling angle (F-ϕ) is shown diagrammatically in Fig. 3c, d, respectively. Dashed green lines represent detachment from the toe side and dashed-dotted blue lines represent detachment from the heel side. The area of the F_N-F_T relation is related to the contact condition.

Stress distribution at the contact changes when the tip shape changes. When the tip shapes contribute to the relaxation of the stress concentration at the edge of the tip, the detachment force increases. In contrast, when they contribute to enhance the stress concentration, the detachment force decreases.

Results and discussion

The detachment condition of devices with different tip shapes was measured for a wide range of pulling angles. The results are represented as F_N-F_T and F-ϕ plots in Fig. 4 in the case of S100%, S125%, and S150% devices. The detachment force increased with the thickness H, (or tip width W), and decreased with the aspect ratio $h/H\ \cos\theta$ (because h is constant). It has been suggested theoretically that the area of the F_N-F_T plots increases with the inverse of the aspect ratio [22], and our results are well described by these models. The results pertaining devices Types 4 and 5 are shown in Figs. 5 and 6. The detachment force slightly increased compared to straight structures with the same W. The detachment force increment was more significant for the region of $\phi > \theta$ than that of $\phi < \theta$, i.e. the stress at the rear edge was more relaxed, in the case of H125%. Conversely, the stress at both side was relaxed about the same in the case of H150%. The stress relaxation at the edge of the tip was likely due to the tip widening, i.e. constricted, generated by the heel structure, which is similar to mushroom-shaped structures [16], albeit less significant. The results of devices T150%, S100%, and S150% are compared in Fig. 7. In the region of $\phi > \theta$ (i.e. detachment from the heel side), T150% exhibit a similar behavior as S100%, whereas in the region of $\phi < \theta$, (i.e., the detachment from the

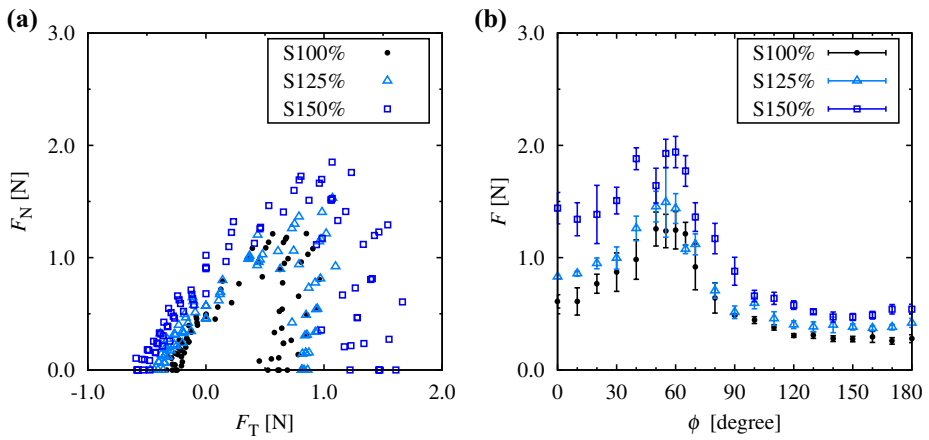

Fig. 4 Experimental results of S100%, S125%, and S150% adhesive devices **a** F_N-F_T relation, and **b** F-φ relation

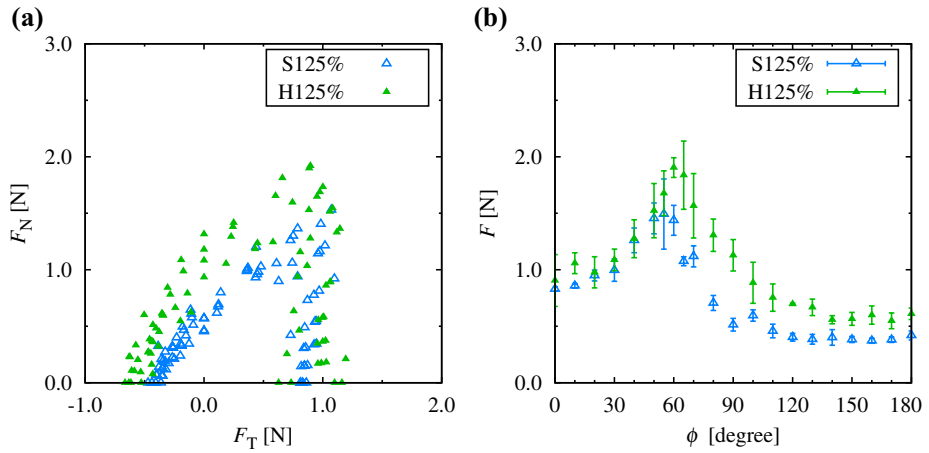

Fig. 5 Experimental results of S125% and H125% adhesive devices **a** F_N-F_T relation, and **b** F-φ relation

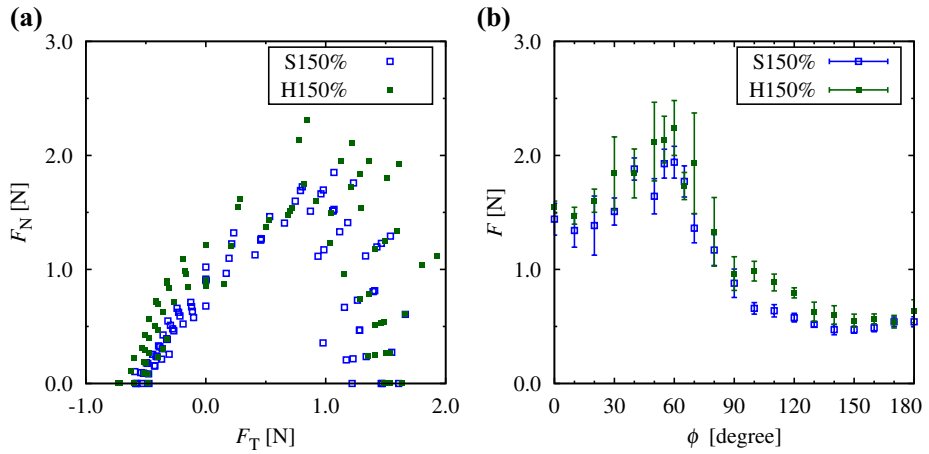

Fig. 6 Experimental results of S150% and H150% adhesive devices **a** F_N-F_T relation, and **b** F-φ relation

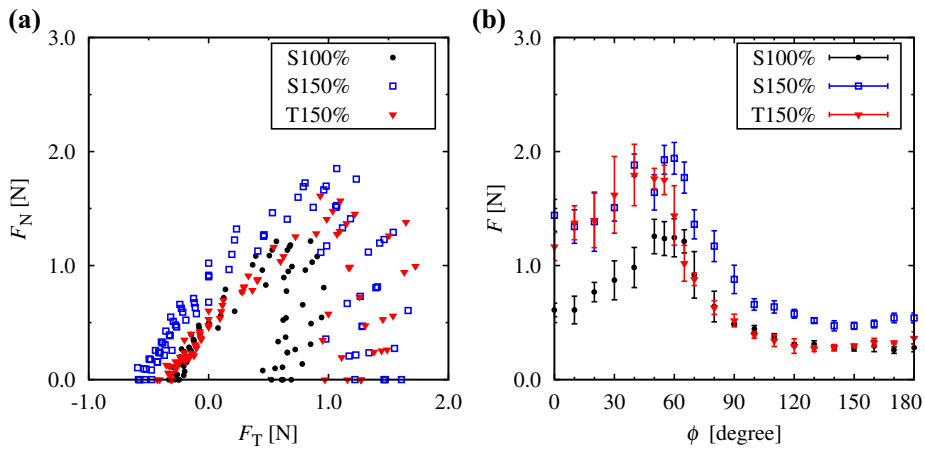

Fig. 7 Experimental results of S100%, S150%, and T150% adhesive devices **a** F_N-F_T relation, and **b** F-φ relation

toe side) the behavior is similar to S150%. Further, the detachment condition shifted in the vicinity of $\phi = \theta$, the asymmetry of the F_N-F_T relation was enhanced, with stronger adhesion in the region $\phi < \theta$ and easier detachment in the region of $\phi > \theta$. It is considered that the stress at the front edge was relaxed due to the toe structure, whereas the stress at the rear edge was not affected because the rear edge structure of T150% is same as that of S100%. Finally, the results of HT175% structure are shown in Fig. 8 compared with the H125% and T150% data. Although the structure of HT175% is the combination of H125% and T150%, the results were more similar to sample H125%, and the effect of the toe elongation was negligible, which indicated that the stress was not relaxed at the front edge. When the force is applied at an angle $\phi < \theta$, the rear edge of the structure can be deformed in the case of T150%. The heel structure, however, prevents it for HT175%. That might be one of the reasons to generate the difference at the detachment force between T150% and HT175% in the region of $\phi < \theta$. Although HT175% has the largest tip size, the maximum detachment force was not increased. These findings suggest that

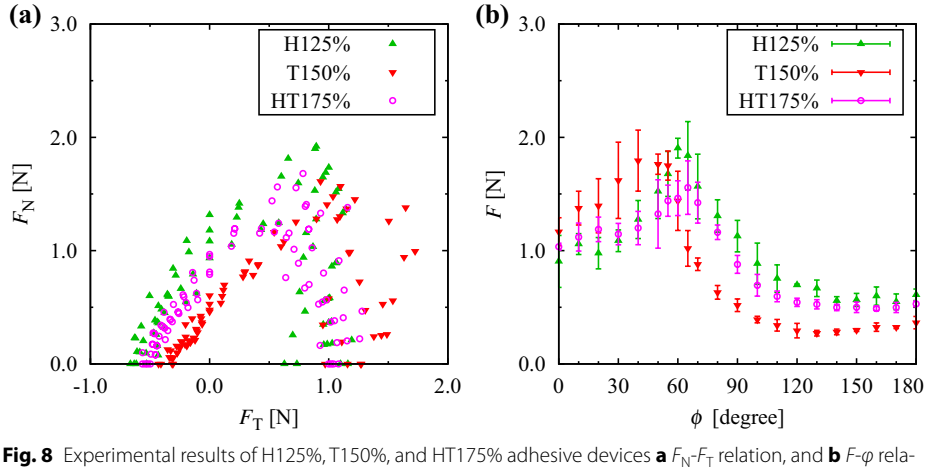

Fig. 8 Experimental results of H125%, T150%, and HT175% adhesive devices **a** F_N-F_T relation, and **b** F-φ relation

the additional tip structures on both side of the tip edges do not promote strong and asymmetric adhesion.

Different from the vertical structures, the oblique structures give rise to an asymmetric detachment. Moreover, the detachment condition can be tuned by varying the tip structure of oblique beam arrays, and the asymmetric property can be changed. Therefore, optimum design of the tip shape has a potential to make more creative adhesive devices in accordance with the intended use.

Conclusions

Adhesive devices consisting of silicone rubber oblique beam arrays were fabricated, and their detachment force was experimentally investigated as a function of the pulling angle. Metallic molds with different tip shapes were used to fabricate different beam tip shapes: straight, heel-like elongation, toe-like elongation, and both heel-like and toe-like elongation.

Detachment occurs when the maximum stress at the contact tip overcomes the limiting stress for adhesion. Although the asymmetric dependence of the normal and tangential forces at the detachment can be obtained with a tilted beam structure, the beam tip shape also affects this dependence. In the case of tips with heel elongation, the overall detachment force increased compared with straight tip structures. In the case of tips with toe elongation, the intensity of the detachment force on the pulling angle and its asymmetry differed from those of the other samples. These findings demonstrate that the anisotropic friction behavior of oblique beam arrays can be enhanced by tuning the geometry of the beam tips.

Authors' contributions
YS carried out the experiments and wrote the manuscript. CS helped writing the manuscript. Both authors read and approved the final manuscript.

Acknowledgements
This work was supported by JSPS KAKENHI Grant Number 15K17933.

Competing interests
The authors declare that they have no competing interests.

Funding
Japan Society for the Promotion of Science (15K17933).

Received: 31 August 2016 Accepted: 22 February 2017
Published online: 09 March 2017

References

1. Hora SL. The adhesive apparatus on the toes of certain geckos and tree frogs. J Proc Asiatic Soc Bengal. 1923;19:137–45.
2. Mahendra BC. Contributions to the bionomics, anatomy, reproduction and development of the Indian house gecko, *Hemidactylus flaviviridis* Ruppel. Part II. The problem of locomotion. Proc Indian Acad Sci. 1941;3:288–306.
3. Maderson PFA. Keratinized epidermal derivatives as an aid to climbing in gekkonid lizards. Nature. 1964;203:780–1. doi:10.1038/203780a0.
4. Russell AP. A contribution to the functional morphology of the foot to the tokay, Gekko gecko (Reptilia, Gekkonidae). J Zool Lond. 1975;176:437–76. doi:10.1111/j.1469-7998.1975.tb03215.x.
5. Autumn K, Liang YA, Hsieh ST, Zesch W, Chan WP, Kenny TW, Fearing R, Full RJ. Adhesive force of a single gecko foothair. Nature. 2000;405:681–5. doi:10.1038/35015073.
6. Walker G. Adhesion to smooth surfaces by insects —a review. Int J Adhes Adhes. 1993;13:3–7. doi:10.1016/0143-7496(93)90002-Q.
7. Gorb SN. Uncovering insect stickiness: structure and properties of hairy attachment devices. Am Entomol. 2005;51:31–5. doi:10.1093/ae/51.1.31.

8. Aksak B, Murphy MP, Sitti M. Adhesion of biologically inspired vertical and angled polymer microfiber arrays. Langmuir. 2007;23:3322–32. doi:10.1021/la062697t.
9. Murphy MP, Aksak B, Sitti M. Adhesion and anisotropic friction enhancements of angled heterogeneous micro-fiber arrays with spherical and spatula tips. J Adhes Sci Technol. 2007;21:1281–96. doi:10.1163/156856107782328380.
10. Parness A, Soto D, Esparza N, Gravish N, Wilkinson M, Autumn K, Cutkosky M. A microfabricated wedge-shape adhesive array displaying gecko-like dynamic adhesion, directionality and long lifetime. J R Soc Interface. 2009;6:1223–32. doi:10.1098/rsif.2008.0048.
11. Jeong HE, Lee JK, Kim HN, Moon SH, Suh KY. A nontransferring dry adhesive with hierarchical polymer nanohairs. Proc Natl Acad Sci USA. 2009;106:5639–44. doi:10.1073/pnas.0900323106.
12. Kwak MK, Pang C, Jeong HE, Kim HN, Yoon H, Jung HS, Suh KY. Towards the next level of bioinspired dry adhesives: new designs and applications. Adv Funct Mater. 2011;21:3606–16. doi:10.1002/adfm.201100982.
13. Jin K, Cremaldi JC, Erickson JS, Tian Y, Israelachvili JN, Pesika NS. Biomimetic bidirectional switchable adhesive inspired by the gecko. Adv Funct Mater. 2014;24:574–9. doi:10.1002/adfm.201301960.
14. Wang Z, Gu P, Wu X. Gecko-inspired bidirectional double-sided adhesives. Soft Matter. 2014;10:3301–10. doi:10.1039/c3sm52921e.
15. Gorb S, Varenberg M, Perssadko A, Tuma J. Biomimetic mushroom-shaped fibrillary adhesive microstructure. J R Soc Interface. 2007;4:271–5. doi:10.1098/rsif.2006.0164.
16. Spuskanyuk AV, McMeeking RM, Deshpande VS, Arzt E. The effect of shape on the adhesion of fibrillary surfaces. Acta Biomater. 2008;4:1669–76. doi:10.1016/j.actbio.2008.05.026.
17. Davies J, Haq S, Hawke T, Sargent JP. A practical approach to the development of a synthetic gecko tape. Int J Adhes Adhes. 2009;29:380–90. doi:10.1016/j.ijadhadh.2008.07.009.
18. Carbone G, Pierro E, Gorb SN. Origin of the superior adhesive performance of mushroom-shaped microstructured surfaces. Soft Matter. 2011;7:5545–52. doi:10.1039/c0sm01482f.
19. Kang SM. Bioinspired design and fabrication of green-environmental dry adhesive with robust wide-tip shape. Int J Precis Eng Manuf Green Technol. 2016;3:189–92. doi:10.1007/s40684-016-0025-3.
20. Takahashi K, Berengueres JOL, Obata KJ, Saito S. Geckos' foot hair structure and their ability to hang from rough surfaces and move quickly. Int J Adhes Adhes. 2006;26:639–43. doi:10.1016/j.ijadhadh.2005.12.002.
21. Hu C, Greaney PA. Role of seta angle and flexibility in the gecko adhesion mechanism. J Appl Phys. 2014;116:074302. doi:10.1063/1.4892628.
22. Sekiguchi Y, Saito S, Takahashi K, Sato C. Flexibility and poisson effect on detachment of gecko-inpired adhesives. Int J Adhes Adhes. 2015;62:55–62. doi:10.1016/j.ijadhadh.2015.06.011.
23. Sekiguchi Y, Takahashi K, Sato C. Adhesion mechanism of a gecko-inspired oblique structure with an adhesive tip for asymmetric detachment. J Phys D Appl Phys. 2015;48:475301. doi:10.1088/0022-3727/48/47/475301.